The manuscript was submitted for possible publication in JPCS (EUCAS issue)

Phase transformations during the reaction heat treatment of Nb_3Sn superconductors

C Scheuerlein[1], M Di Michiel[2], L Thilly[3], F Buta[4], X Peng[5], E Gregory[6], J A Parrell[7], I Pong[1], B Bordini[1], M Cantoni[8]

[1] European Organization for Nuclear Research (CERN), 1211 Geneva 23, Switzerland
[2] European Synchrotron Radiation Facility (ESRF), 38000 Grenoble, France
[3] University of Poitiers, PHYMAT (UMR 6630 CNRS), 86962 Futuroscope, France
[4] University of Geneva, 1211 Geneva 4, Switzerland
[5] Hyper Tech Research Inc., Columbus, OH, 43210, USA
[6] Supergenics LLC I, Jefferson, MA, 01522, USA
[7] Oxford Superconducting Technology, Carteret, NJ, 07008, USA
[8] Ecole Polytechnique Fédérale de Lausanne (EPFL), Switzerland

Corresponding author: Christian.Scheuerlein@cern.ch

Abstract. The evolution of Nb containing phases during the diffusion heat treatment of three different high critical current Nb_3Sn strand types is compared, based on synchrotron X-ray diffraction results that have been obtained at the ID15 beam line of the European Synchrotron Radiation Facility (ESRF). In all strands studied, Nb_3Sn formation is preceded by the formation of a Cu-Nb-Sn ternary phase, $NbSn_2$ and Nb_6Sn_5. As compared to the PIT and Tube Type strand, the amount of these phases formed in the RRP strand is relatively small. In the RRP strand subelements with a fine filament structure Nb_3Sn grows more quickly, thereby preventing to a large extent the formation of the other higher tin phases.

1. Introduction

During the diffusion heat treatment (HT) of Nb_3Sn superconductors the precursor elements form various intermetallic phases and finally the superconducting Nb_3Sn [1]. The formation of Nb containing phases prior to Nb_3Sn nucleation and growth can degrade the microstructural and microchemical homogeneity in the fully reacted strand, and it is therefore of interest to investigate how the strand design and the overall elemental composition of its sub-elements influence these transformations.

High energy synchrotron X-ray diffraction is an excellent tool for monitoring phase transformations in Nb_3Sn strands during *in-situ* reaction HT's. Previously we have reported the phase transformations that occur in a low loss Nb_3Sn strand [2], a PIT strand [3] and a RRP strand [4]. Here we compare the phase transformations that occur in the RRP and PIT strand with those in a Tube Type Nb_3Sn strand. In order to allow for a semi-quantitative comparison of the phase evolutions, synchrotron diffraction measurements were performed for the three high critical current (J_c) strand types with identical experimental settings.

2. Experimental

Cross sections of the Restacked Rod Process (RRP®) strand [5] produced by Oxford Superconducting Technology, the Powder-in-Tube (PIT) strand [6] produced by Shape Metal Innovation (now part of Bruker EAS) and the Tube Type strand [7] from Hyper Tech Research are presented in figure 1. The nominal diameter of the PIT B215 strand is 1.25 mm. In order to allow for a semi-quantitative comparison of the diffraction results and to investigate the influence of the subelement size, diffraction measurements have also been performed with a PIT B215 strand that has been drawn down to ∅= 0.80 mm. The nominal non-Cu volume fractions in the RRP, Tube Type and PIT strands are 51.9 %, 45.1 % and 46.5 %, respectively. For the Tube Type strand the atomic fractions within the subelements are 4.35 at.% Cu, 21.9 at.% Sn and 73.3 at.% Nb [8]. For the other samples the exact composition of the subelements is not known.

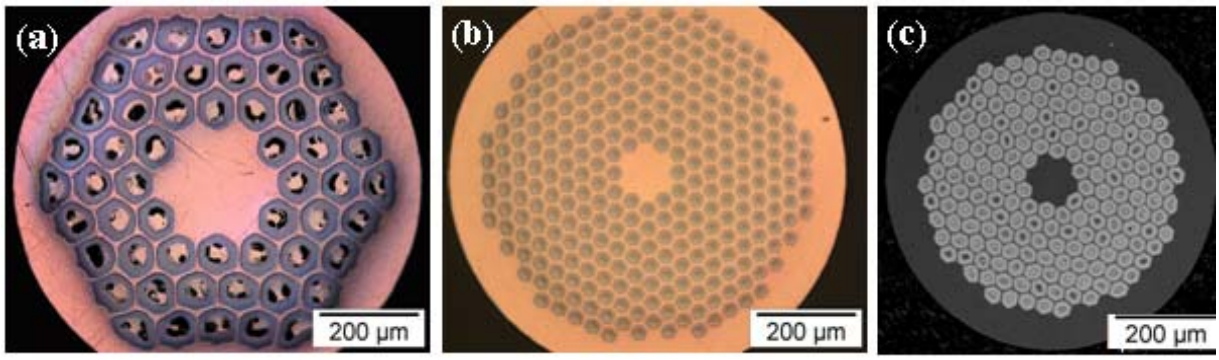

Figure 1: Cross sections of the three strand samples investigated, (RRP billet #7419 with 54 subelements, ∅=0.80 mm, non-Cu=51.9 vol.% (a), PIT B215, with 288 subelements, ∅=0.80 mm, non-Cu=45.1 vol.% (b), and Tube Type T1505 with 192 subelements, ∅=0.70 mm, non-Cu=46.5 vol.% (c)).

The phase transformations in the different strand samples were monitored by high energy (~90 keV) synchrotron X-ray diffraction measurements. During the *in-situ* HT with a temperature ramp rate of 100 °C/h and a 4 h-700 °C isothermal holding step, diffractograms were acquired every 5 minutes. HTs were performed in a dedicated X-ray transparent furnace built at ID15 that enables an accurate sample temperature control during the diffraction experiments. For more information about the diffraction experiment refer to [3]. The present experiment has been optimised for high angular resolution, on the expense of the recorded lattice spacing (*d*-spacing) range. The radially integrated diffractograms acquired for the Tube Type, PIT and RRP strands during *in-situ* HT at 480 °C are shown in figure 2.

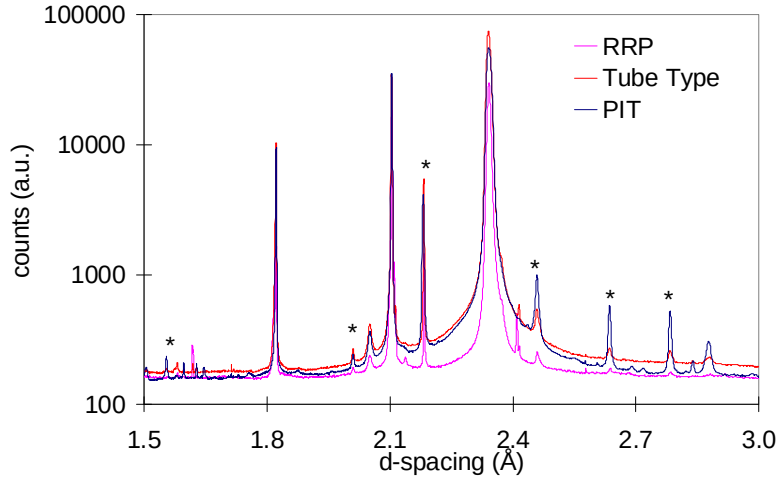

Figure 2: Diffractograms of the RRP, Tube Type and PIT strand acquired during *in-situ* HT at 480 °C. The diffraction peaks that have been assigned to a Cu-Nb-Sn phase are labeled with an asterisk.

The colour intensity plot shown in figure 3 summarizes the 130 diffractograms that were acquired during the reaction HT of the Tube Type strand. A semi-quantitative description of the evolution of all Nb containing phases as a function of temperature has been obtained by monitoring the area of characteristic diffraction peaks. In figure 3 the reflections that have been selected for peak area measurements are labelled in red. Prior to peak area measurements diffractograms were normalized to the X-ray flux reaching the sample, in order to correct for fluctuations of the Synchrotron beam current during the experiment. Diffraction peak areas obtained for the 1.25 mm diameter PIT strand are significantly smaller than those for the 0.8 mm PIT strand, due to the stronger X-ray self absorption in the larger diameter strand sample. In order to facilitate a comparison between the diffraction data of the 1.25 mm diameter strand with that of the other samples, all PIT-1.25 mm data has been multiplied by an arbitrarily chosen factor of 3.

Since the non-Cu volume in the RRP strand exceeds the non-Cu volume in the tubular strands, the peak area comparisons may somewhat overestimate the phase content in the RRP strand with respect to that in the tubular strands.

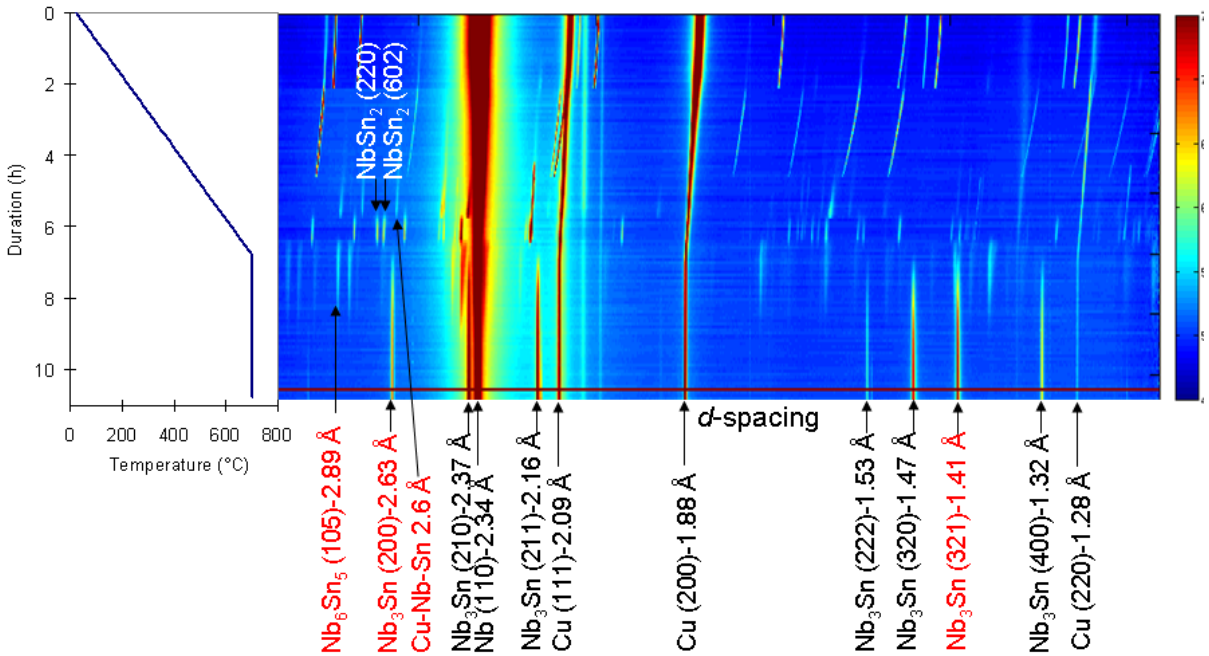

Figure 3: Colour intensity plot summarising 130 diffractograms that have been acquired during *in-situ* HT of the Tube Type Nb_3Sn strand with a ramp rate of 100 °C/h and an additional 4 h-700 °C isothermal step. The reflections that were used for peak area measurements are labeled in red and white. The *d*-spacing axis is inversed with respect to figure 2.

3. Results

3.1. Cu-Nb-Sn ternary phase formation

Formation of at least one Cu-Nb-Sn ternary phase has been observed previously in RRP [9] and later in a PIT strand [3]. As shown in figure 2 characteristic Cu-Nb-Sn diffraction peaks are also detected during the diffusion HT of the Tube Type strand at 480 °C. The Cu-Nb-Sn phase evolution in the three strand types is compared in the left plot of figure 4. Most Cu-Nb-Sn is formed in the PIT strand, probably mostly in the initial powder core. By analytical Transmission Electron Microscopy it can be shown that in the PIT strand some Cu-Nb-Sn is also formed at the inside of the pre-cursor tube [10].

For the RRP strand the Cu-Nb-Sn evolution during the HT without holding steps (this experiment) is compared with the Cu-Nb-Sn growth during a HT with additional 2 h-390 °C and 2 h-482 °C isothermal holding steps, which has been reported in [4]. Because of different experimental settings the peak areas obtained with both experiments can not be compared. However, it can be seen that isothermal holding steps, in particular above the Cu_6Sn_5 decomposition temperature of 415 °C, can promote the formation of Cu-Nb-Sn.

3.2. $NbSn_2$ formation

The $NbSn_2$ evolution in the different strand types is compared in the right plot of figure 4. Similar amounts of $NbSn_2$ are formed in the PIT and Tube Type strands. In the RRP strand less $NbSn_2$ is formed and the temperature interval during which the amount of $NbSn_2$ exceeds the detection limit is relatively small. The Cu-Nb-Sn and $NbSn_2$ peak area evolutions in the PIT strand with 1.25 mm and 0.80 mm diameter are similar.

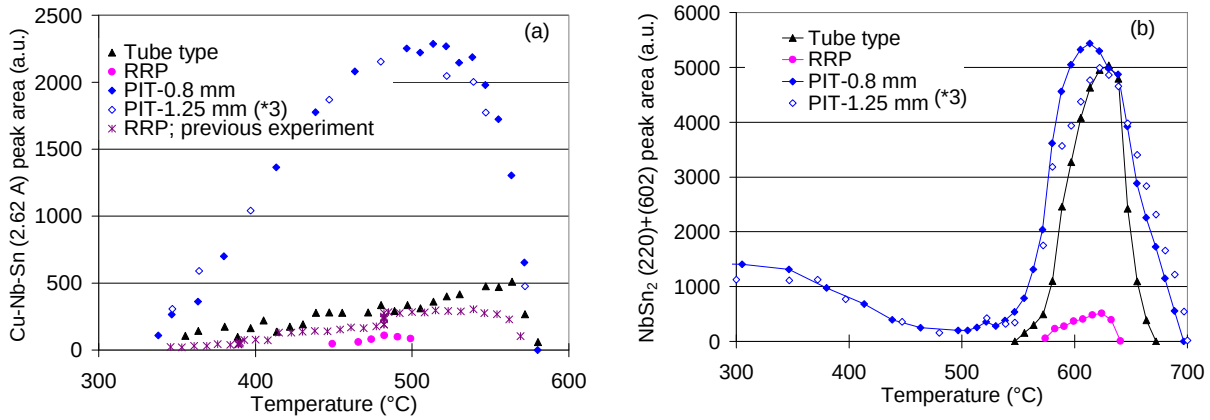

Figure 4: Cu-Nb-Sn (*d*-spacing=2.62 Å) (a) and $NbSn_2$ (220)+(602) peak area (b) evolution in the different strand samples during a 100 °C/h HT. The peak areas of the PIT-1.25 mm strand have been multiplied by a factor of 3.

3.3. Nb_6Sn_5 formation

The Nb_6Sn_5 phase evolution as a function of temperature and HT duration is presented in figure 5. Similar amounts of Nb_6Sn_5 are detected in the PIT and Tube Type strand, whereas a relatively smaller amount of Nb_6Sn_5 is formed in the RRP strand. The temperature and duration after which Nb_6Sn_5 starts to decompose in the different strand types differ significantly.

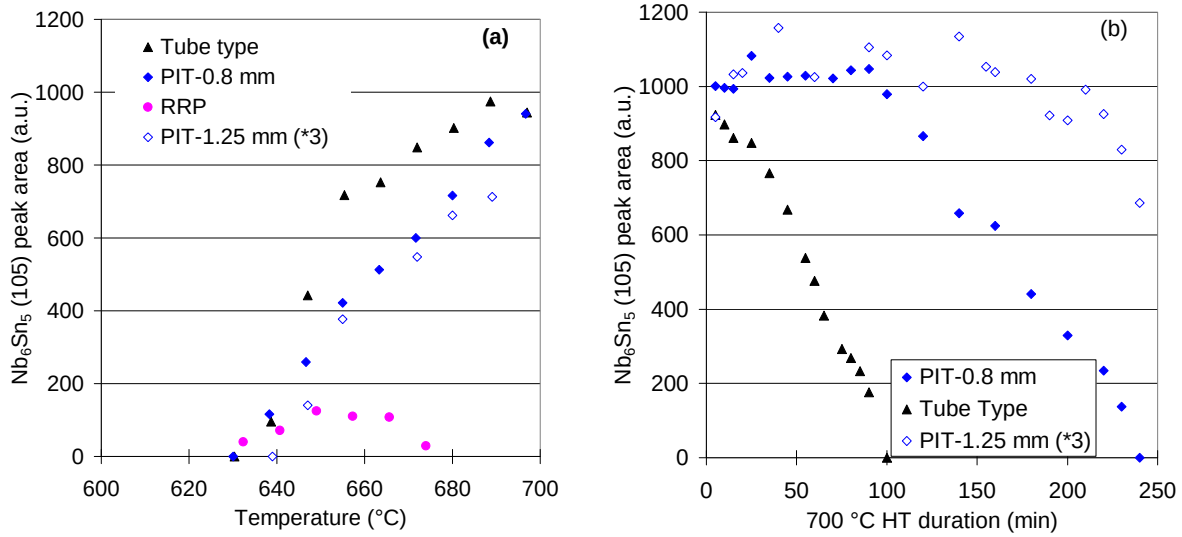

Figure 5: Nb_6Sn_5 (105) peak area as a function of temperature (a) and as a function of 700 °C HT duration (b). The peak areas of the PIT-1.25 mm strand have been multiplied by a factor of 3.

3.4. Nb_3Sn formation

In the RRP strand Nb_3Sn growth is detected at comparatively low temperature (at 510 °C and 530 °C for (200) and (321) oriented Nb_3Sn reflections, respectively). In the PIT and Tube Type strands Nb_3Sn is detected at significantly higher temperatures and, contrary to the RRP strand, for PIT and Tube Type strands Nb_3Sn (321) reflections are observed at a lower temperature than the Nb_3Sn (200) reflections.

In figure 6 the Nb_3Sn growth during a 4 h-700 °C HT is compared for the 3 strand types (left) and for the 0.80 mm and 1.25 mm PIT strand (right). In the RRP strand the Nb_3Sn grains detected have predominantly a (200) orientation, while in the PIT and Tube Type strand they exhibit mostly a (321) orientation parallel to the strand drawing axis. The difference in Nb_3Sn (321) to Nb_3Sn (200) intensity ratio between the RRP strand and the tubular strands is also observed after complete reaction of the different strand types.

In the RRP strand the 700 °C HT duration needed for a complete reaction is roughly 10 h, while in the tubular strand types significantly longer HT durations are needed to achieve a complete reaction at 700 °C.

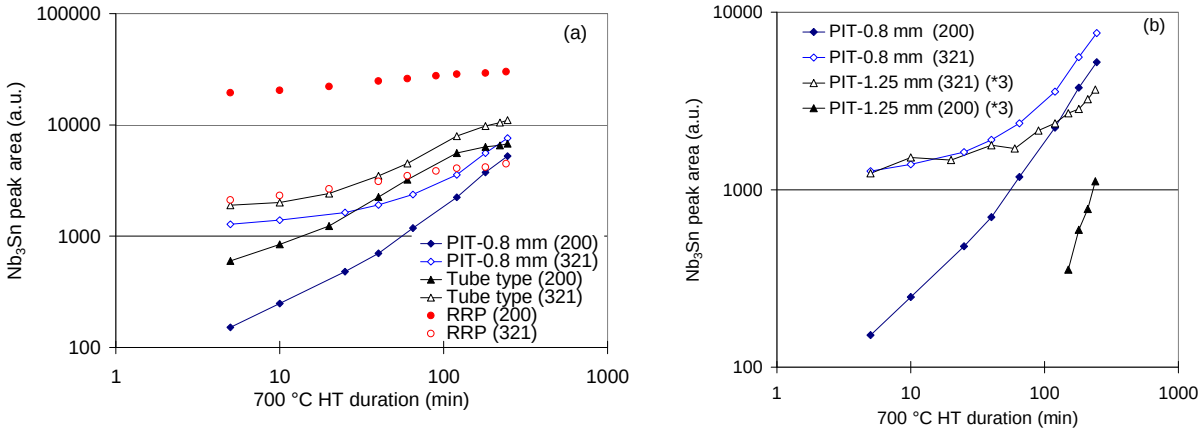

Figure 6: Comparison of Nb_3Sn (200) and (321) peak area evolution vs. 700 °C HT duration for the 3 different strand types (a) and for PIT-1.25 and PIT-0.80 (b). The peak areas of the PIT-1.25 mm strand have been multiplied by a factor of 3.

4. Discussion

The three Nb containing phases Cu-Nb-Sn, $NbSn_2$ and Nb_6Sn_5 are detected during the reaction HT of all high J_c strand types studied. The maximum amount of these phases is comparatively small for the RRP strand and the temperature interval during which the phase quantity exceeds the detection limit is relatively short. In the RRP strand Nb_3Sn growth is detected at about 100 °C lower temperature than it is in the PIT strand, Nb_3Sn growth proceeds faster as in the tubular strand types (see temperature intervals summarized in table 1). It is therefore assumed that fast formation of Nb_3Sn is advantageous for limiting the formation of the higher-tin Nb phases.

Table 1: Approximate temperature intervals in which the amount of Cu-Nb-Sn, $NbSn_2$, Nb_6Sn_5 and Nb_3Sn in the different strand types exceeds the detection limit of the diffraction experiment. *In the PIT strand $NbSn_2$ particles are present in the non-heated strand. **Measured during previous experiment with different experimental settings and temperature cycle; slightly above the detection limit in the present experiment.

	Cu-Nb-Sn	$NbSn_2$	Nb_6Sn_5	Nb_3Sn (200)	Nb_3Sn (321)
SMI-PIT B215 0.8 mm	**340 °C-580 °C**	**(RT-*) ~540-690°C**	**630°C-4h-700 °C**	**>690 °C**	**> 610 °C**
SMI-PIT B215 1.25 mm	**350 °C-570 °C**	**(RT-*) ~540-700°C**	**640°C->4h-700 °C**	**>700 °C**	**>650 °C**
Tube Type T1505	**360 °C-580 °C**	**550 °C-670 °C**	**630°C-1.5 h-700 °C**	**>680 °C**	**>580 °C**
OI-ST RRP (#7419)	***345 °C-575 ° C ******	**570 °C-640 °C**	**630 °C–675 °C**	**>510 °C**	**>530 °C**

From metallographic examination of PIT strand cross sections after full reaction HT [11] it is known that approximately 25 % of the total Nb_3Sn volume is made of coarse grain Nb_3Sn, which is formed upon Nb_6Sn_5 decomposition. The diffraction data shown in figure 5 suggests that the amount of Nb_6Sn_5 formed in the RRP strand is not more than 20 % of that formed in the PIT strand. The relatively small amount of Nb_6Sn_5 formed in the RRP strand explains at least partly the J_c differences between the RRP and tubular strand types, assuming that the current is only conducted in the Nb_3Sn that is formed by solid state diffusion of Sn into the Nb precursor, but not in the Nb_3Sn formed upon decomposition of the higher Sn-phases.

A comparison of the Cu-Nb-Sn phase evolution in the RRP strand during HT with and without isothermal holding steps (see figure 4) indicates that prolonged HT duration below the Cu-Nb-Sn decomposition temperature promotes the growth of the Cu-Nb-Sn phase.

Reducing the tube cross sectional area in the PIT B215 strand by a factor of 2.4 does not have a strong influence on the Cu-Nb-Sn and $NbSn_2$ phase evolution and the temperature intervals during which these phases are detected (see figure 4). In contrast, the Nb_3Sn formation kinetics and the duration needed to transform Nb_6Sn_5 entirely into Nb_3Sn are significantly influenced by the subelement size.

The results presented in Figure 6 suggest that the Nb_3Sn grain orientation distribution in a fully reacted RRP strand differs strongly from that observed in the tubular strand types. Powder diffraction data gives a Nb_3Sn (321) to Nb_3Sn (200) intensity ratio of 3 in isotropic Nb_3Sn, but intensity ratios reported here can not be directly compared to published powder diffraction data since only a fraction of the diffraction rings has been recorded with the present experimental set-up.

Texture analysis of a PIT strand similar to the one studied here [12] shows that the strong <110> Nb-Ta texture that develops as a consequence of the severe cold drawing of the precursor tubes, is not modified by the reaction HT, and as a result of the initial texture of the Nb-Ta precursor, in the PIT strand the Nb_3Sn grains grow also with a preferential <110> orientation parallel to the strand axis. Further texture analysis of the precursor and Nb_3Sn in RRP strands is needed in order to understand the reasons for the different Nb_3Sn grain orientation distribution in the different strand types.

5. Conclusion

In all three high J_c strand types studied, Nb_3Sn formation is preceded by the formation of at least one Cu-Nb-Sn ternary phase, $NbSn_2$ and Nb_6Sn_5. In the RRP subelements Nb_3Sn forms more quickly, preventing to a large extent the formation of the other higher-tin phases, and explaining at least partly why at present highest J_c values are achieved with the RRP type strands.

Acknowledgements

We acknowledge the ESRF for beam time on ID15.

References

[1] M. T. Naus, P. J. Lee, and D. C. Larbalestier, "The interdiffusion of Cu and Sn in internal Sn Nb Sn superconductors," IEEE Trans. Appl. Supercond., 10(1), (2000) 983–987

[2] C. Scheuerlein, M. Di Michiel, A. Haibel, "On the formation of voids in Nb_3Sn superconductors", Appl. Phys. Lett., 90, 132510, (2007)

[3] M. Di Michiel, C. Scheuerlein, "Phase transformations during the reaction heat treatment of powder-in-tube Nb_3Sn superconductors", Supercond. Sci. Technol. 20, (2007) L55-L58

[4] C. Scheuerlein, M. Di Michiel, G. Arnau, F. Buta, "Phase transformations during the reaction heat treatment of Internal Tin Nb_3Sn strands with high Sn content", IEEE Trans. Appl. Supercond. 18(4), (2008), 1754-1760

[5] J. A. Parrell, Y. Zhang, M.B. Field, P. Cisek, S. Hong, "High Field Nb_3Sn Conductor Development at Oxford Superconducting Technology", IEEE Trans. Appl. Supercon. 13(2), (2003), 3470-3473

[6] T. Boutboul1, L. Oberli1, A. den Ouden, D. Pedrini, B. Seeber, G. Volpini, IEEE Trans. Appl. Supercond. 19(3), (2009), 2564-2567

[7] E. Gregory, M. Tomsic, X. Peng, M.D. Sumption, A. Ghosh, "Nb_3Sn superconductors made by an economical tubular process and other techniques," IEEE Trans. Appl. Supercond. 18(4), (2008),

[8] S. Bhartiya, M.D. Sumption, X. Peng, E. Gregory, M.J. Tomsic, E.W. Collings, "Investigation of the Effects of Low Temperature Heat Treatments on the Microstructure and Properties of Multifilamentary, Tube-Type Nb_3Sn Strands", IEEE Trans. Appl. Supercond. 19(3), (2009), 2588-2592

[9] M. T. Naus, P. J. Lee, and D. C. Larbalestier, "The influence of the starting Cu–Sn phase on the superconducting properties of subsequently reacted internal-Sn Nb Sn conductors," IEEE Trans. Appl. Supercond., 11(1), (2001), 3569–3572

[10] M Cantoni, C Scheuerlein, P-Y Pfirter, F de Borman, J Rossen, G Arnau, L Oberli, P Lee, "Sn concentration gradients in Powder-in-Tube superconductors", Proceedings of EUCAS'09, submitted.

[11] M. Fischer, "Investigation of the Relationships Between Superconducting Properties and Reaction Conditions in Powder-In-Tube Nb_3Sn Conductors", MSc thesis, University of Wisconsin, (2002)

[12] C. Scheuerlein, U. Stuhr, L. Thilly, "In-situ neutron diffraction under tensile loading of powder-in-tube Cu/Nb_3Sn composite wires: effect of reaction heat treatment on texture, internal stress state and load transfer", Appl. Phys. Lett., 91(4), 042503, (2007)